Int. J. Heat Mass Transfer. Vol. 8, pp. 729–748. Pergamon Press 1965. Printed in Great Britain

HEAT TRANSFER TO TURBINE BLADING IN THE PRESENCE OF SECONDARY FLOW

L. A. WALKER* and E. MARKLAND†
The Universities of Newcastle and Nottingham

(*Received* 4 *September* 1964 *and in revised form* 30 *October* 1964)

Abstract—As part of a study of heat transfer to gas turbine blading, local heat-transfer coefficients were measured round chordwise profiles of one blade of a cascade when heated to a few degrees above the air stream temperature, each measuring profile being made isothermal in turn. The flow at inlet had boundary layers artificially thickened by spoilers to about one third of the blade span, so that strong secondary flows were set up in the deflecting stream.

Over the uniform-flow region at the centre of the span results are shown to be virtually two-dimensional. Comparison with the earlier work of Wilson and Pope [1] shows some differences, particularly at zero incidence. One important mechanism by which variation of total pressure along the span may increase the heat transfer is by forward movement of the boundary-layer transition to the site of a local pressure reversal near the leading edge of the section, under conditions when, with two-dimensional flow, the layer would remain laminar after the pressure reversal. A further effect is the contribution of the spanwise velocities at the blade surface, produced by secondary flows, which increase heat transfer and skin friction. The resulting increase in mean heat-transfer rate due to the severe non-uniformity of upstream conditions was 6 per cent at design incidence.

Measurements of secondary flow made in the blade passages were compared with calculations of various degrees of refinement based on methods due to Hawthorne [2] and to Squire and Winter [3]. The correlation is reasonably good in all cases.

NOMENCLATURE

c, blade chord;

Cp, $= 1 - \left(\frac{U_{xz}}{U_{2z}}\right)^2$;

h, heat-transfer coefficient;

k, thermal conductivity of air;

m $= \frac{P_{xz}}{P_{1c}}$;

Nu, Nusselt number $= \frac{hc}{k}$, $\overline{Nu}$, mean Nusselt number, $Nu_x = \frac{hx}{k}$;

p, static pressure;

P, total pressure;

Re, Reynolds number;

$Re_2 = \frac{U_{2c}c}{\nu}$, $Re_{2z} = \frac{U_{2z}c}{\nu}$, $\overline{Re}_2 = \frac{\bar{U}_{2c}}{\nu}$, $Re_x = \frac{U_{xz}x}{\nu}$;

U, mainstream velocity;

$\bar{U}$, mean of U;

v, w, induced components of velocity in y- and z-directions;

x, y, z / X, Y, Z, co-ordinates defined in Fig. 4.

μ, ν, absolute, kinematic viscosity.

Suffixes

1, upstream condition;

1c, upstream condition at midspan;

2, downstream condition;

2c, downstream condition at midspan;

xz, condition at point (x, z) of blade surface;

2z, condition at point in downstream plane at which the streamline passing over point (x, z) intersects the downstream plane.

* Department of Mechanical and Marine Engineering, University of Newcastle.

† Department of Mechanical Engineering, University of Nottingham.

INTRODUCTION

THERE HAS been no dearth of literature to recommend the use of turbine inlet temperatures higher than those at present possible with gas turbine installations. Brown [4] showed, for instance, that the effect of raising the operating temperature from 1250°F to 2200°F in a typical two shaft set with intercooling and heat exchanger but no reheat would raise the efficiency from 33·5 to 46 per cent and reduce the specific mass flow from 62 to 22 lb/h.p. h. Ainley [5] has stated the case for the jet turbine, where in one example for an aircraft flying at Mach number 0·75 an increase in specific thrust of 40 per cent was calculated with a 360 degF rise in turbine inlet temperature above 1340°F for a slight reduction in the specific fuel consumption. The improvements in compactness are clearly substantial.

The practical limitation on turbine inlet temperature is placed by the physical properties of the blade material, particularly the requirements of low creep and high strength at elevated temperature, and resistance to thermal shock. Cooling the blades raises the permissible gas temperature for a given material; Ainley [6] reports full-scale tests on an experimental turbine operating at over 2000°F with air-cooled blades. Whether or not the blades are cooled, knowledge of local heat-transfer coefficients is desirable to determine thermal gradients within the blade as well as the total heat input to a cooled blade.

Wilson and Pope [1] investigated the distribution of heat-transfer coefficient round the profile of a blade in cascade using surface heating strips. Ainley [6], however, showed that heat transfer to a blade of an operating turbine is substantially higher than for a blade in a stationary cascade. There are a number of factors which may contribute to this increase. The stream turbulence following combustion, the centrifugal effect on the boundary layer, and the secondary flow engendered by non-uniform conditions in the flow approaching the turbine blades may all contribute. The present tests were aimed at investigating the last of these factors, and involved detailed measurements of secondary flow and of heat-transfer coefficients at the surface of a stationary blade in cascade, when the approaching stream had a considerable velocity gradient in the spanwise direction.

AIRFLOW AND CASCADE ARRANGEMENT

The blower tunnel and cascade was that used by Wilson and Pope [1] with suitable modification made to the airstream, cascade and instrumentation.

Blower power limitations to 40 h.p. resulted in a five blade cascade of 10 in span made to the profile given in Fig. 1—effectively a six-fold scale increase of a 1-in chord prototype. The blades were cast in plaster, apart from the heated one mounted in the centre, and were set in cascade at the outlet of the blower tunnel. Cascade rotation allowed a range of stream incidence from −30 to +20 degrees about the zero design value.

The stream approaching the cascade was confined between fixed side walls at the ends of

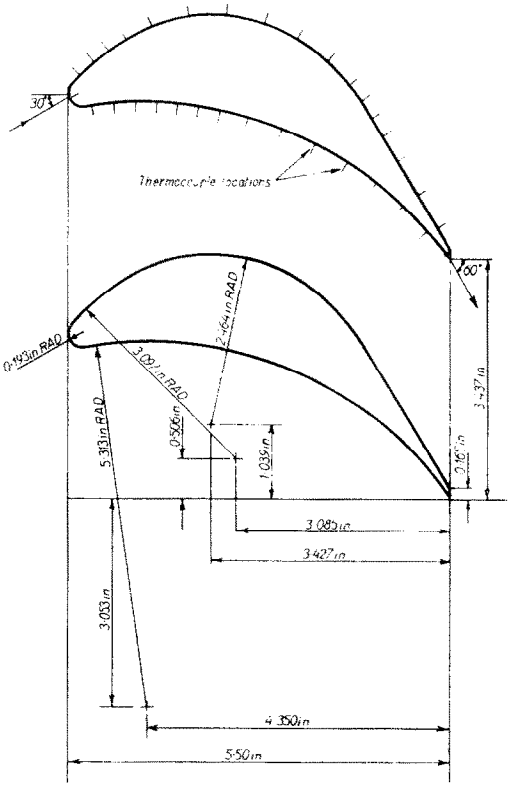

FIG. 1. Cascade geometry and blade profile.

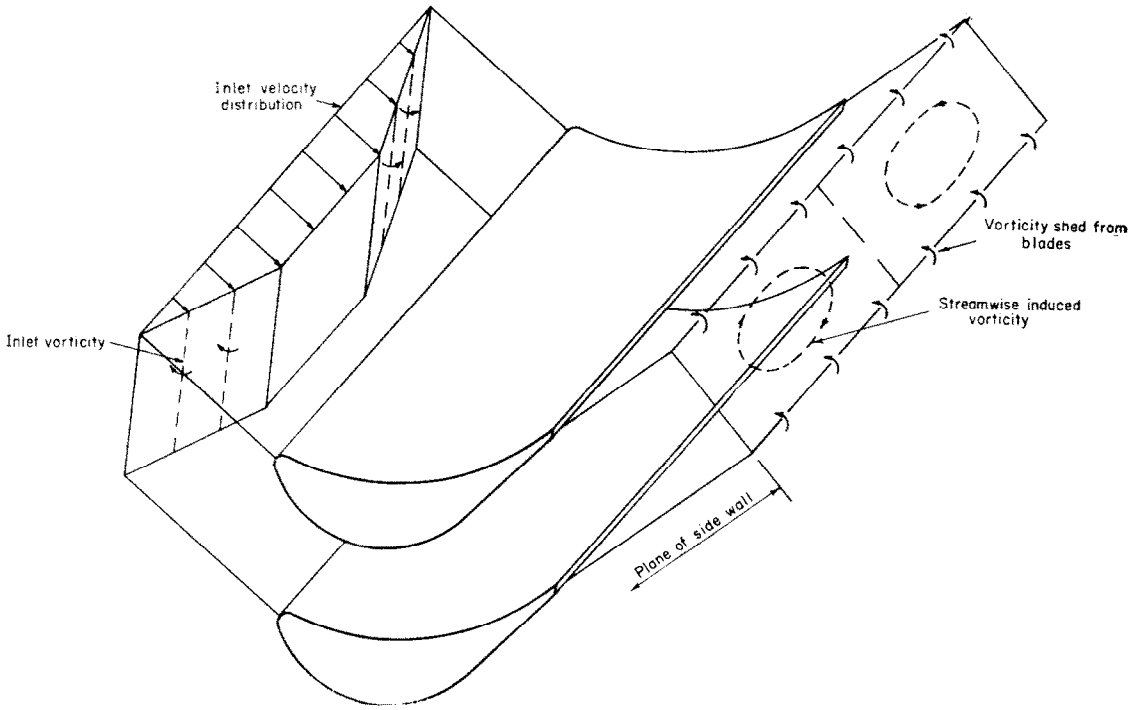

FIG. 2. Nature of stream deflexion.

the blade span and upper and lower walls shaped to contract the airflow from the exit of the main tunnel contraction to the height of the cascade, different shapes being used for the different incidences chosen. The four walls continued for one chord length downstream of the trailing edges, the upper and lower walls being adjustable in direction. By adjusting the exit direction and by applying suction over a zone of holes 6 in upstream of the leading edges, uniform conditions were produced in the direction of the cascade, as shown by static pressure measurements over the upstream traverse plane and by static pressure tappings on the plane side walls 1 in upstream of the leading edges. The upstream traverse plane was $\frac{3}{4}$ chord length ahead of the plane of the leading edges; a pitot-static pair and claw type yawmeter could be traversed to any point in the plane.

MEASUREMENT WITHIN THE BLADE SPACES

The direction of flow at points within the space between blades was found using the special yawmeter shown diagrammatically in Fig. 3. Rotation of the instrument in a bearing at the side wall provided measurement of angle in the (xy) planes. This rotation is about an axis parallel to lines of leading edges. Rotation of the instrument in the (xz) plane (i.e. measurement of yaw angle) was effected by a parallelogram linkage similar to that used by Todd [7]; movement of a link outside the cascade produced displacement of the two instrument stems which were linked to the instrument head in the airstream. This movement did not displace the point of measurement. The head could be traversed to any spanwise station by a lead screw, and could be traversed on a slide in the Y direction in any of the 5 planes shown in Fig. 4.

A correction to recorded angles was made to allow for the error introduced by the total pressure gradient of the stream, the total pressure distribution being obtained from a Pitot tube mounted centrally in the yawmeter tube assembly. The instrument was calibrated

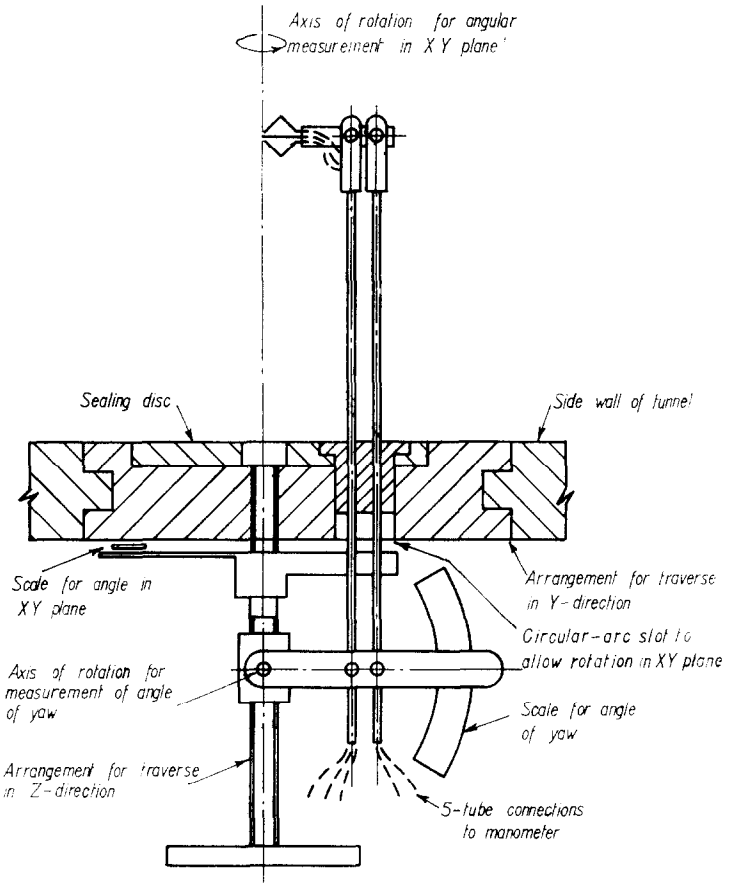

FIG. 3. Diagram of special yawmeter.

at the exit of a long duct having a square section of 3 in side mounted with its axis parallel to the tunnel airstream.

BLADE FORM

Figure 1 gives the blade profile and cascade geometry. This is the same cascade as that used by Wilson and Pope [1], and conveniently provides pressure gradients favourable to the growth of laminar boundary layers at some incidences. The profile is known as T.6, having a camber and setting typical of a 50 per cent reaction blade. At zero incidence, inlet and and outlet angles are 30 and 60 degrees respectively. The data relevant to its aerodynamic testing at N.G.T.E. are given by Bridle [8].

WIND TUNNEL DEVELOPMENTS

Some preliminary changes were made to the wind tunnel, as originally used, to improve the regularity of the flow at entry to the cascade. Substantial variations in angle and velocity over planes C and D (Fig. 5) were traced to boundary-layer separation at the diffuser entry plane A, which was cured by installing $\frac{3}{8}$ in cell bakelized paper honeycomb in the diffuser neck B; further smoothing was achieved by using similar honeycomb in the settling section at C_1. Coarse and fine wire gauzes were fitted at planes C_2 and C_3. The resulting velocity profile at plane D was uniform in magnitude to $\pm 0{\cdot}7$ per cent and variations in flow angle were within the limits $+2°$ and $-4°$.

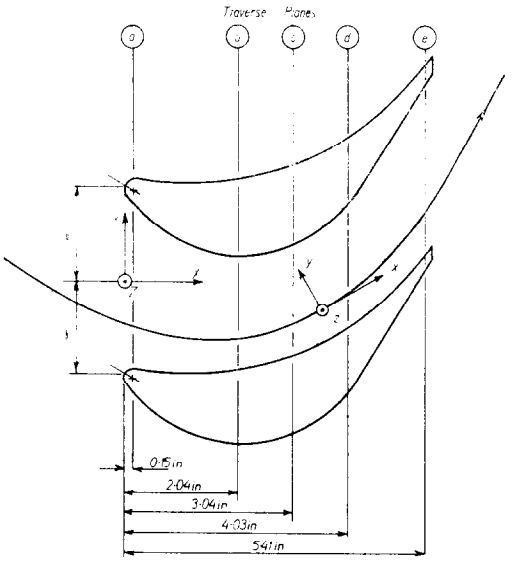

FIG. 4. Co-ordinate systems and traverse planes between blades.

PRODUCTION OF TOTAL PRESSURE PROFILE

Artificial thickening of the wall boundary layer downstream of plane D was made by flow spoilers of $\frac{1}{4}$ in cell honeycomb mounted at D, some 5–6 chords upstream of the blades. The cell axes ran parallel to the stream and the honeycomb section was cut with a taper towards the mid-span of the blades. Overlapping strips of wire gauze mounted on the upstream face of the honeycomb added further obstruction nearer to the wall, and after some trials the conditions of Fig. 6 at the inlet plane E were produced. Velocity gradations were regular, but changes in the angle of incidence (or pitch) inevitably occurred owing to the variation of bound blade circulation along the span. This variation was detected at the upstream traversing plane, which was not sufficiently far upstream of the leading edges to be uninfluenced by conditions which are inseparable from any lifting surface in a non-uniform stream.

THE PRESSURE BLADE

Measurements of static pressure around the profile were made at the centre blade of the cascade at 26 orifice tappings around the contour. The tappings were made in semi-stiff nylon tubes sealed at their inoperative ends and cast in the blade. A single metal spar held the tubes in correct relationship to the blade surface, to define a single chordwise profile of holes, which were quite flush with the blade profile. The system was leakproof and gave a rapid response.

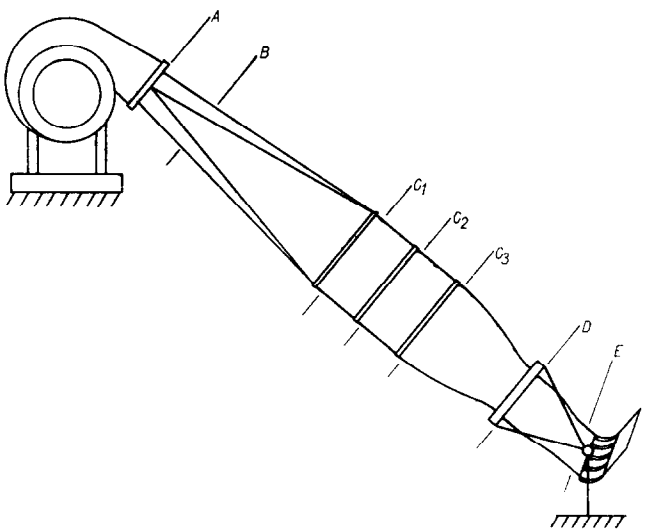

FIG. 5. Arrangement of cascade wind tunnel.

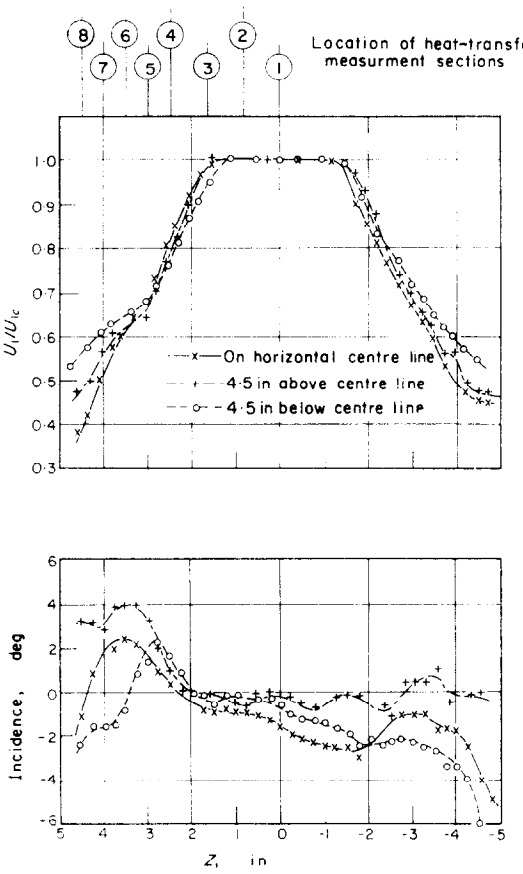

FIG. 6. Velocity and angle traverses at inlet plane.

THE HEATER BLADE

Heat-transfer measurements were made using a special heated blade which could be inserted in lieu of the pressure-measuring blade at the central position of the cascade. This blade was an accurately made model in spruce wood (chosen for its low thermal conductivity). The surface was shellaced and covered with metal foil strips. The first two layers to be bonded, in order, were narrow flat thermoelement strips of copper and of constantan of 0·002 in thickness. The strips ran spanwise, and were separated by the resin insulator base of the outer foils. Thermojunctions were made at desired spanwise locations by removing this resin and soldering the adjacent copper and constantan foils together. Finally the heater surfaces in 0·004 in constantan were mounted with each strip lying centrally over a thermoelement. Electrical insulation between layers was of the order of 2 MΩ, indicating also a low thermal conductivity between surface and blade interior. The 32 heater foils were of variable width to provide concentration of data in regions of rapidly varying heat-transfer rate, e.g. at the leading edge and convex surface transition region.

Great care was taken to achieve aerodynamic smoothness, particularly near the leading edge, which was covered by a single strip. The gaps between strips were filled by a mixture of filler and bonding agent, smoothed off with solvent. The positions of the thermoelements determined the locations of local heat-transfer measurements round the profile, and by sliding the blade across the tunnel through sealed apertures in the side walls, successive measurements could be made to cover the whole blade surface. The air seal at the points where the blade passed through the walls was effected by shaped clamps with rubber cushions. Local overheating of the heating elements where they passed through the wall was prevented by thermal shunts.

There was in fact a limitation to the extent of the travel, imposed by the available lengths of etched foils, which necessitated two rows of thermocouples around the blade, so that heat-transfer readings could be obtained over the blade semi-span with a travel of only $\frac{1}{4}$-span. It was fortunately possible to check the consistency of readings obtained from the two sets of thermoelements by traversing each of them in turn to the same spanwise position (station 4); under all conditions good agreement was found.

The heaters were supplied from a stabilized 2 V d.c. source, with individual currents controlled by slide wire resistors and measured by recording the potential across a resistance in series with the heater. Blade thermocouples were connected in turn via a telephone uniselector to a reference junction and the e.m.f. measured by potentiometer. Reference junctions were provided at the ice point, at the upstream total temperature, in the wake, and in the blade interior.

Figure 7 illustrates the heater and pressure blades.

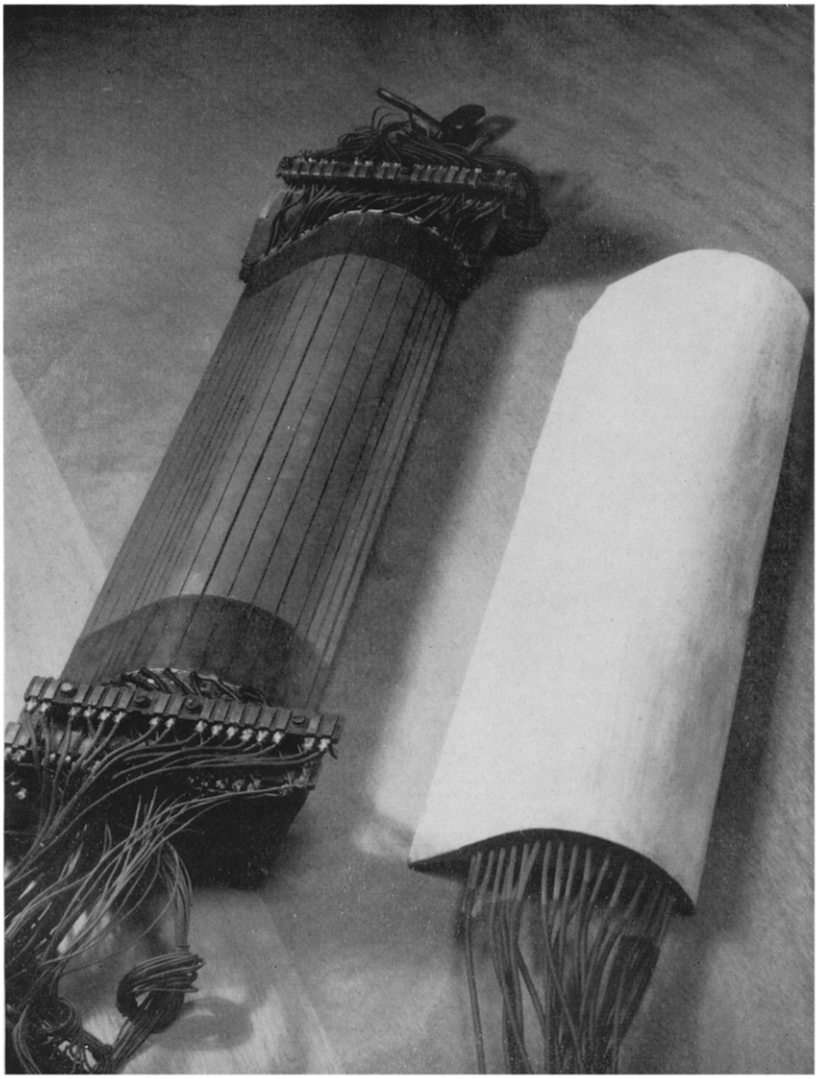

FIG. 7. Heater and pressure blades.

[*facing page* 734]

AIRFLOW MEASUREMENTS

Over the inlet plane the velocity distribution is roughly trapezoidal in the spanwise direction, being uniform over the middle third, and varying linearly from the walls over the outer thirds. A description of the secondary flows generated, as indicated on Fig. 2, has been given by Carter [9]. They have an influence on surface static-pressure coefficients which is considered below in two parts, viz: (*a*) over the uniform region near the centre and (*b*) over the outer one-third spans.

(*a*) Over the central region the differences are slight between pressure coefficients measured with the trapezoidal inlet profile and with those measured under conditions of two-dimensional flow, (which, incidentally, agree well with a potential flow solution for the cascade). The differences arise from the fact that the measured static pressure drop is slightly smaller when the inlet velocity profile is non-uniform, an effect which is due to the reduction of stream deflection through the cascade caused by secondary flow. This exceeds the tendency towards an increased pressure drop caused by a contraction of the uniform stream width seen from consideration of continuity and momentum. A converse net stream contraction effect has been noticed by Stuart [10] where a superimposed acceleration occurred in a

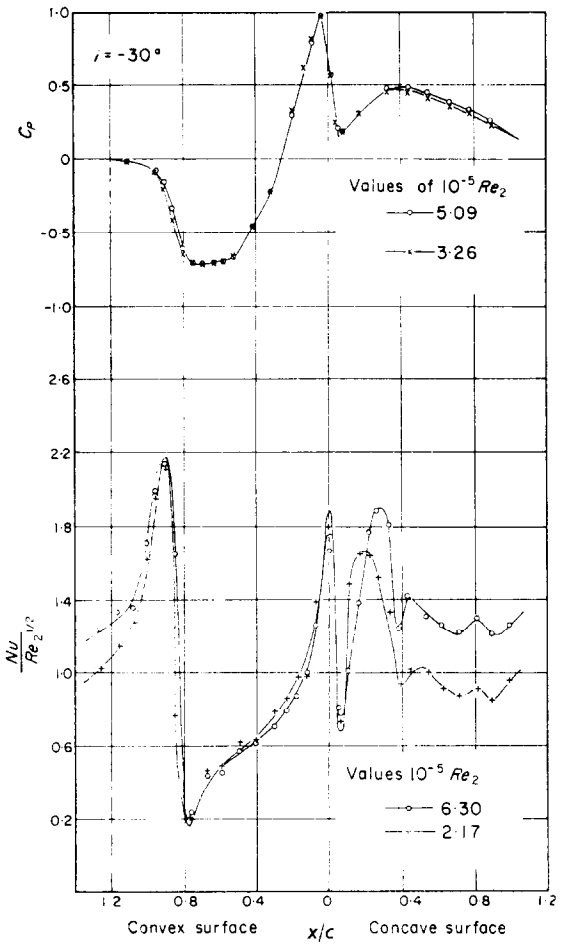

FIG. 8. Two-dimensional static-pressure and heat-transfer coefficients −30° incidence.

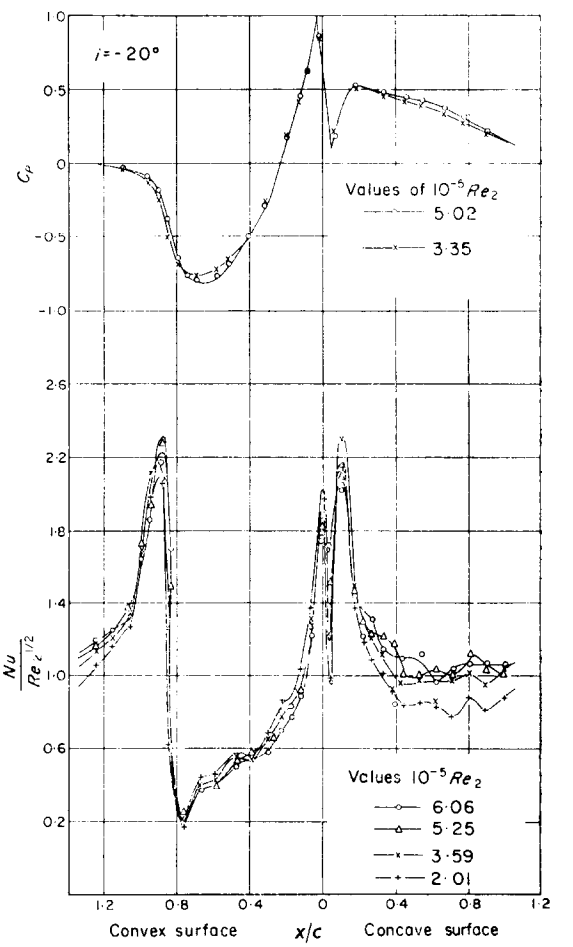

FIG. 9. Two-dimensional static-pressure and heat-transfer coefficients −20° incidence.

compressor cascade due to relatively thin boundary layers at inlet.

(*b*) In the region of non-uniform profile there is an additional influence on pressure coefficients. The induced cross velocities displace streamlines near the convex blade surface towards the centre of the span, and those near the concave surface towards the side walls. This causes the local velocity at a given position to differ from its two-dimensional value since the total pressure in the relevant streamline will not be the same as that in the same spanwise station upstream.

Figures 8–13 show static pressure and heat-transfer coefficients measured at the centre span position for a range of speeds and incidences; corresponding results at other stations in the region of total pressure variation (selected from the range of tests) are shown in Figs. 14–19.

The pressure coefficient Cp is plotted against x/c where x is measured along the surface from the design stagnation point. Cp at any point (xz) on the blade surface is defined by

$$Cp = 1 - \left(\frac{U_{xz}}{U_{2z}}\right)^2 = 1 - \frac{P_{xz} - p_{xz}}{P_{2z} - p_{2z}}$$

in which the suffix xz denotes local conditions at the point and $2z$ denotes conditions in the downstream plane at the point where the streamline just outside the boundary layer at (xz) intersects

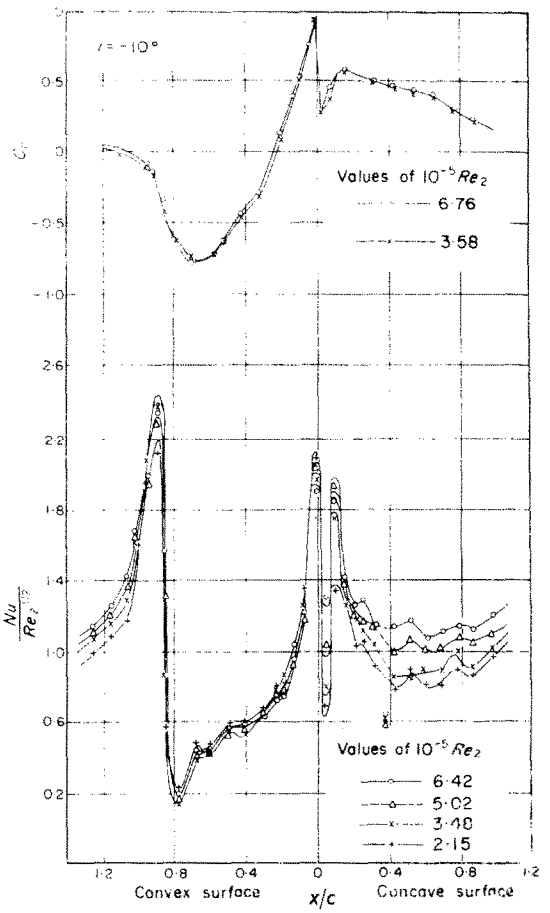

FIG. 10. Two-dimensional static-pressure and heat-transfer coefficients −10° incidence.

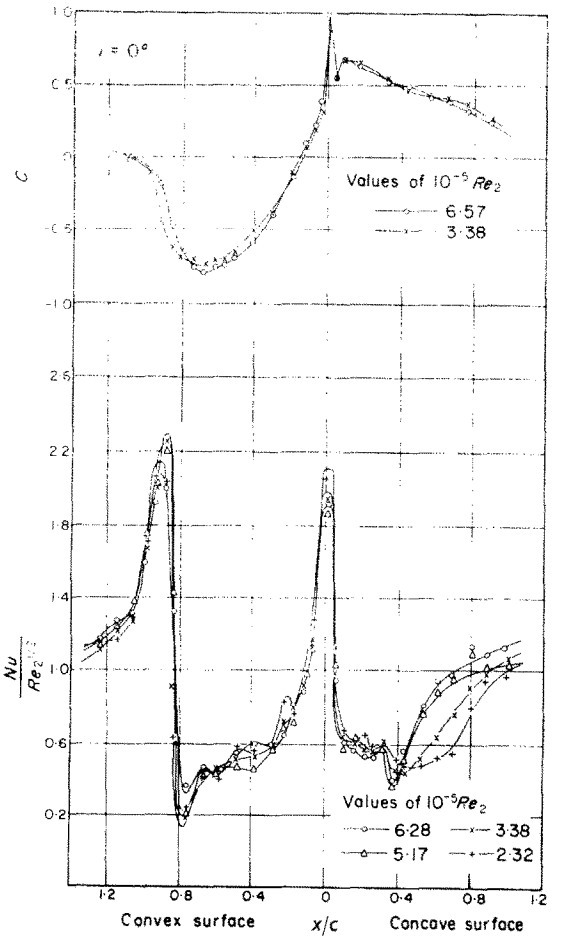

FIG. 11. Two-dimensional static-pressure and heat-transfer coefficients 0° incidence.

this downstream plane. (In general, this occurs at a different value of z because of the displacement of the flow caused by secondary velocities). p_{2z} takes on the uniform atmospheric pressure p_2 for all values of Y and z, and P_{2z} is equal to P_{xz}, so Cp may be rewritten

$$Cp = \frac{p_{xz} - p_2}{P_{xz} - p_2}$$

If P_{xz} is expressed in terms of the upstream total pressure at midspan P_{1c} by $P_{xz} = mP_{1c}$

then

$$Cp = \frac{p_{xz} - p_2}{mP_{1c} - p_2}$$

Values of m are plotted, for one of the incidences used, as a function of x and z in Fig. 20.

SECONDARY FLOW BETWEEN BLADES

The sideways deflection of the stream as it passes through the blade passages may be considered in two parts. Firstly there is the displacement due to spanwise pressure gradients arising from the acceleration of the non-uniform flow through the passages which may be calculated approximately by the actuator disk theory [11].

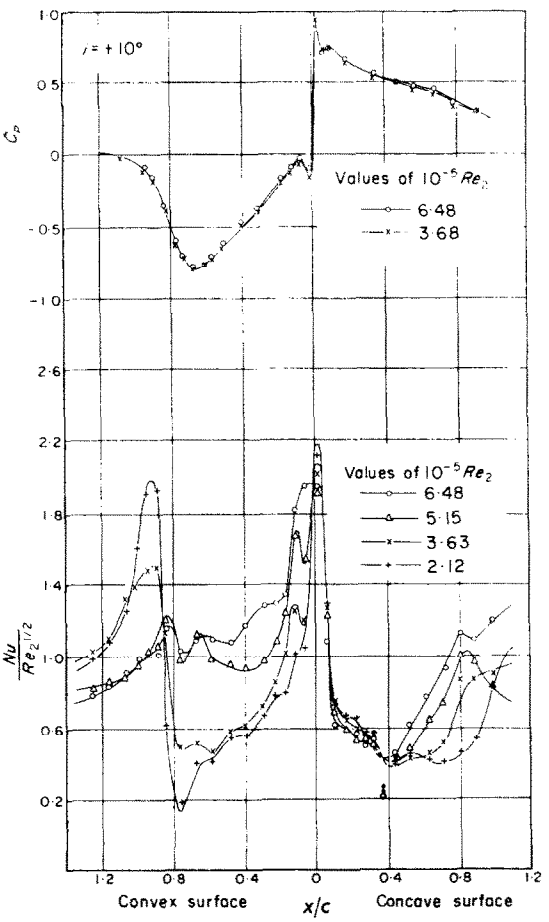

FIG. 12. Two-dimensional static-pressure and heat-transfer coefficients +10° incidence.

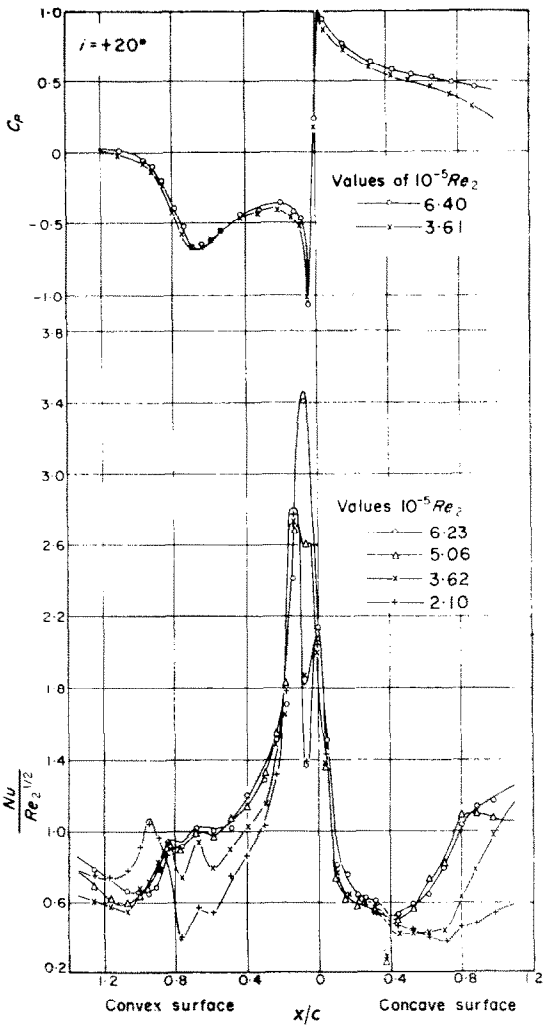

FIG. 13. Two-dimensional static-pressure and heat-transfer coefficients +20° incidence.

This may be regarded as the primary flow field. Then there are cross-components of velocity arising from the streamwise component of vorticity generated within the blade passages; these components are added to the primary field with the assumption that it is thereby not appreciably perturbed. The two-dimensional potential flow has been calculated by relaxation method so there is the possibility of calculating secondary flows produced by the known upstream velocity profile by a number of methods, viz:

(*i*) *Hawthorne's method* [2]

(a) with a primary field assumed to be two-dimensional with velocities in each of the (*xy*) planes assumed to be in simple proportion to upstream velocity in each plane.

(b) with a primary field derived from comparison between measured velocities in the blade passages with those of the two-dimensional potential solution. There is, however, great difficulty in measuring static pressure in a highly rotational stream, so that velocities can be measured reliably only over upstream and downstream planes where the flow is unperturbed, and over the blade surfaces. Taking the measured and potential velocity fields in a given (*xy*) plane to coincide at the

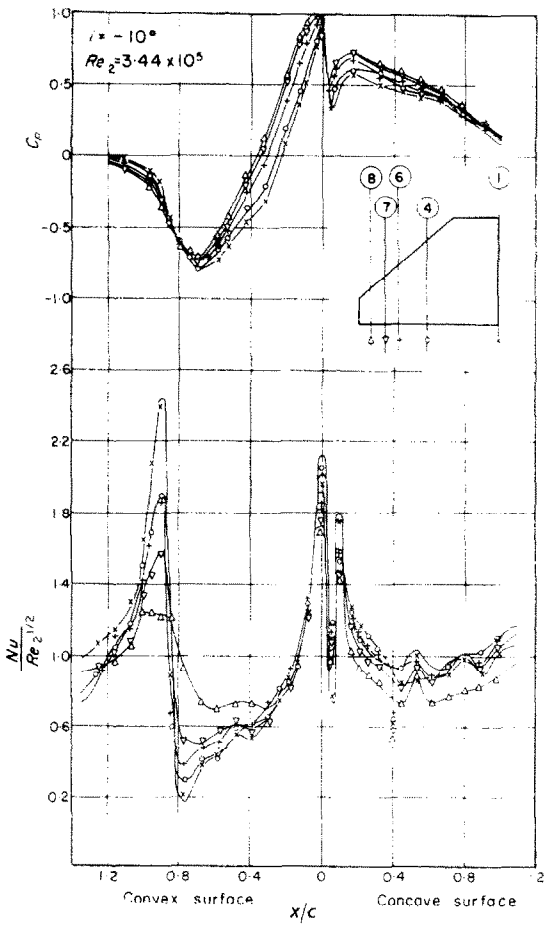

FIG. 14. Static-pressure and heat-transfer coefficients along blade span −10° incidence, $Re_2 = 3{\cdot}44 \times 10^5$.

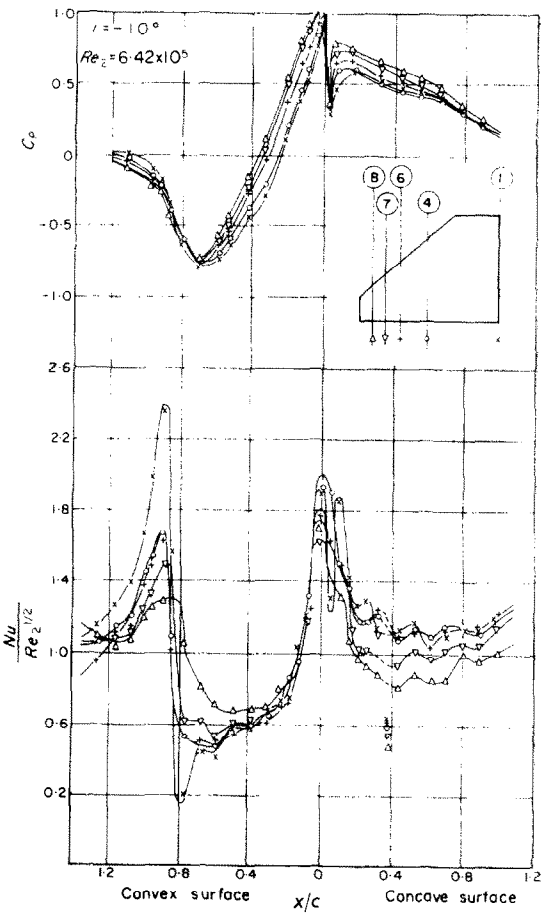

FIG. 15. Static-pressure and heat-transfer coefficients along blade span −10° incidence, $Re_2 = 6{\cdot}42 \times 10^5$.

downstream plane, the differences which exist between them may be expressed in terms of differences in pressure coefficients along the blade surfaces and the upstream plane. Suitable corrections may then be applied to match the potential solution to the measured values. By interpolation corrections within the blade passage space may then be found. Thus the velocty at any point of the flow is inferred from measurement, which gives the required information for deducing the primary field.

(ii) Squire and Winter's method [3]

Comparison of results of calculation with measurements taken at a typical measuring plane within the blade passage is made on Figs. 21 and 22. The components of velocity v and w shown on these figures have been derived from angles measured by the special yawmeter of Fig. 3 and from velocities inferred by the method described above. It is hoped to present details of the calculations at a later date, but it is interesting to note here that the refinement of Hawthorne's method as compared with that of Squire and Winter does not lead to significantly better agreement with experiment. The correction of the primary field, which involves measurements on the blade surfaces, and considerable additional calculation, produces no significant

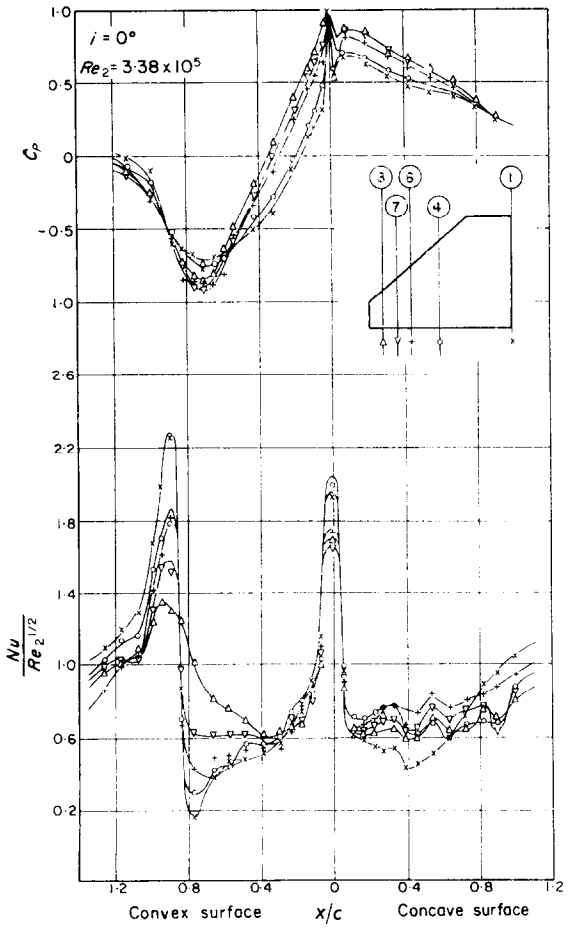

FIG. 16. Static-pressure and heat-transfer coefficients along blade span 0° incidence, $Re = 3{\cdot}38 \times 10^5$.

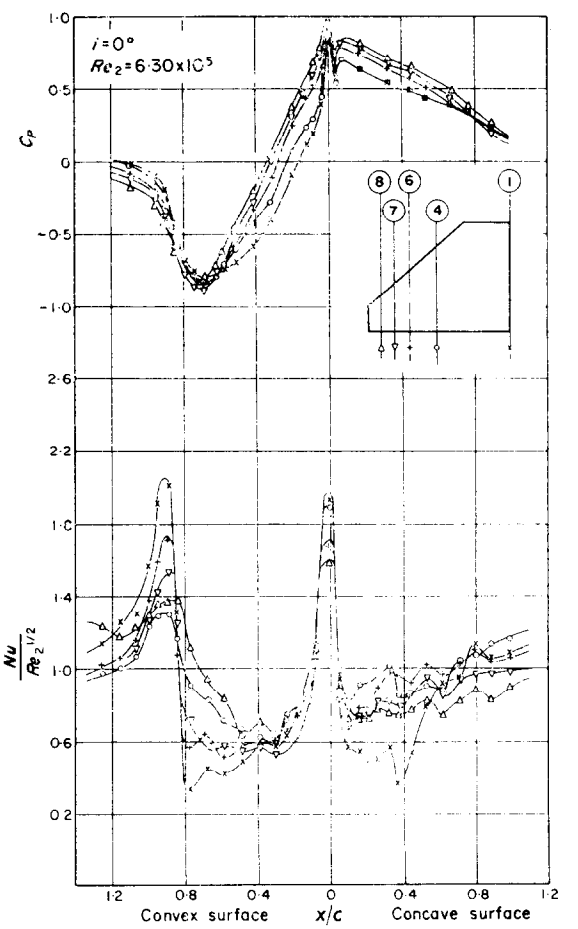

FIG. 17. Static-pressure and heat-transfer coefficients along blade span 0° incidence, $Re_2 = 6{\cdot}30 \times 10^5$.

improvement. It should be borne in mind that the experimental velocity components depend on inferred primary velocities in the blade passage, and that the calculations are made first in planes normal to the direction of flow, and then transferred to the traverse planes of Fig. 4.

HEAT-TRANSFER MEASUREMENTS

The local Nusselt number Nu_x for laminar flow of a fluid at constant Prandtl number over a flat plate in zero pressure gradient is related to the local Reynolds number Re_x by

$$Nu_x = \lambda(Re_x)^{\frac{1}{2}}$$

where λ is a constant [12]. Over a curved surface with pressure gradient, changes in the velocity profile make λ dependent on x. For a blade of chord c in a cascade of specified geometry subject to non-uniform inlet flow (so that U_x/U_2 is a function of x/c and z), local values of Nu and Re may conveniently be expressed in terms of c and of downstream velocity U_2, so that

$$\frac{Nu}{(Re_2)^{\frac{1}{2}}} = f(x/c, z)$$

where $f(x/c, z)$ is determined by measurement. Provided the boundary layer is laminar, $f(x/c, z)$ will be independent of Re_2, i.e. of speed. Regions of turbulent boundary layer will be revealed by

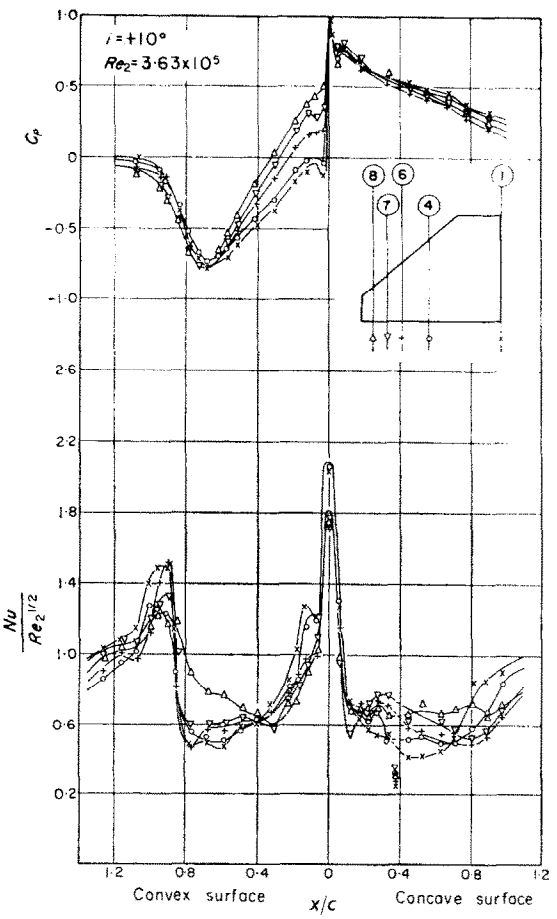

FIG. 18. Static-pressure and heat-transfer coefficients along blade span +10° incidence, $Re_2 = 3{\cdot}63 \times 10^5$.

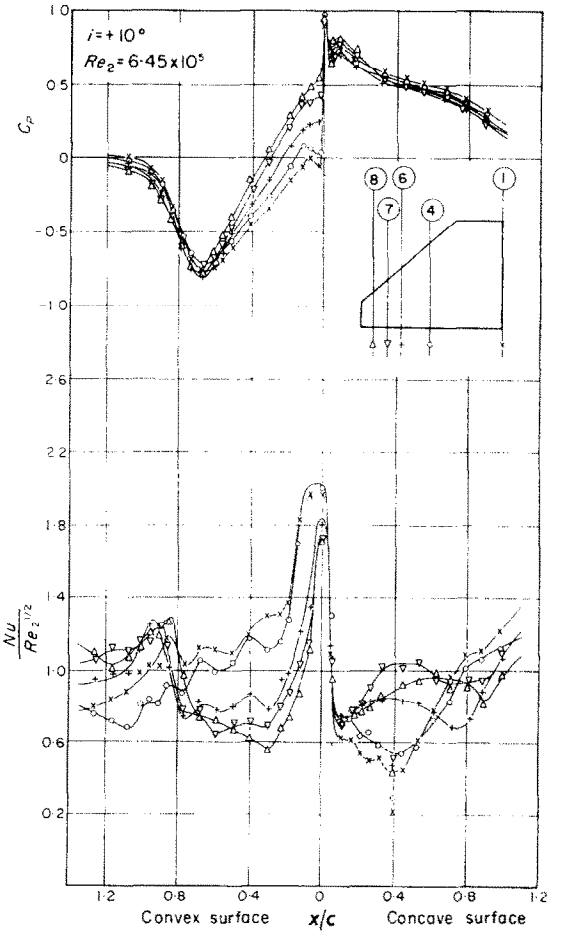

FIG. 19. Static-pressure and heat-transfer coefficients along blade span +10° incidence, $Re_2 = 6{\cdot}45 \times 10^5$.

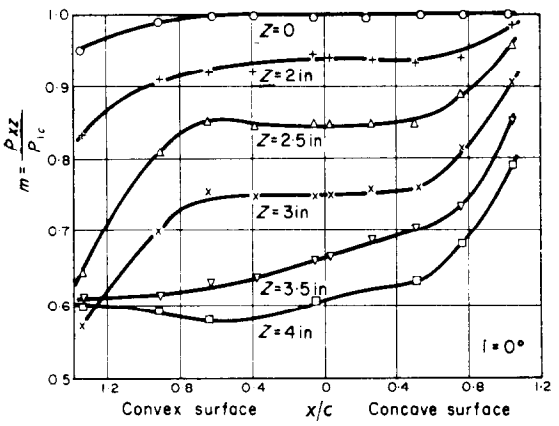

FIG. 20. Distribution of total pressure over blade, 0° incidence.

a dependence of $f(x/c, z)$ on speed since the square root relation between Nu and Re_2 no longer applies.

Several possibilities are open for the choice of downstream velocity on which to base Re when there is spanwise velocity variation. In the presentations of Figs. 8–19 the midspan velocity U_{2c} has been used, so that the value of $Nu/(Re_2)^{\frac{1}{2}}$ at a point in the regions of reduced velocity towards the ends of the span is lower than if it were based on a downstream velocity appropriate to the point in question. However, the coefficient is in terms of data most likely to be available to the designer, and affords a direct comparison with two-dimensional results. Conversion of $Nu/(Re_2)^{\frac{1}{2}}$ to $Nu/(Re_{2z})^{\frac{1}{2}}$, where Re_{2z} is based on the downstream velocity U_{2z} appropriate to a chosen point on the blade surface, is effected by

$$\frac{Nu}{(Re_{2z})^{\frac{1}{2}}} = m^{-\frac{1}{2}} \frac{Nu}{(Re_2)^{\frac{1}{2}}}.$$

Conversion to $Nu_x/(Re_x)^{\frac{1}{2}}$ where the dimensionless expressions are based on local co-ordinate x and local speed U_{xz}, is obtained by

$$\frac{Nu_x}{(Re_x)^{\frac{1}{2}}} = \left(\frac{x}{c}\right)^{\frac{1}{2}} [m(1 - Cp)]^{-\frac{1}{2}} \frac{Nu}{(Re_2)^{\frac{1}{2}}}$$

subject to the convention that p_2, the downstream pressure, be taken as a zero datum. The distribution of m over the surfaces may be inferred from measurements of total pressure such as those presented on Fig. 20; measurements of Cp are shown in Figs. 14–19. A discussion of overall mean heat-transfer rates is given at a later stage.

THERMAL RATIO AND TEMPERATURE DIFFERENCE

The ratio of blade surface to air temperature is about 1·03 in the experiments; for a turbine blade it is less than unity and for a cooled blade it may typically be 0·8. Andrews and Bradley [13] found that the overall heat-transfer coefficient of a blade in cascade is sensibly independent of temperature ratio over the range

$$1{\cdot}5 \times 10^5 < Re < 7{\cdot}0 \times 10^5$$

provided that gas density is based on the mean of inlet and outlet pressures, and temperature on the mean of blade and stagnation temperatures. A second influence of temperature ratio has been examined by Lees [14] who demonstrated the improved stability of a laminar boundary layer as the surface to gas temperature ratio is reduced. The data of the present tests were reduced by computing local values of Nu and Re using the gas properties k and μ chosen at the blade temperature. Density was taken at the downstream value, in view of its negligible change across the cascade.

For a given blade geometry Eckert and Weise [15] have shown that

$$Nu = f\{Re, Pr, M, \Delta t_{ad}/(t_w - t_s)\}$$

where Δt_{ad} is the dynamic temperature interval in an adiabatic process and t_w and t_s are respectively the wall and gas static temperatures. The value of h, on which Nu depends, deduced from $q = hA(t_w - t_s)$ therefore depends on the temperature ratio within f. It may be shown, [16], that dependence of h on the interval $(t_w - t_s)$ is removed if t_s is replaced by the kinetic temperature $t_k = t_s + (rU^2/2gCpJ)$ where r is the recovery factor. In these tests r was taken as 0·85 throughout, although strictly it would require a slightly higher value (0·89) for a turbulent layer. The maximum error would be about 0·1 degC in the highest-speed case of 250 ft/s, or 1 per cent of the interval $(t_w - t_k)$.

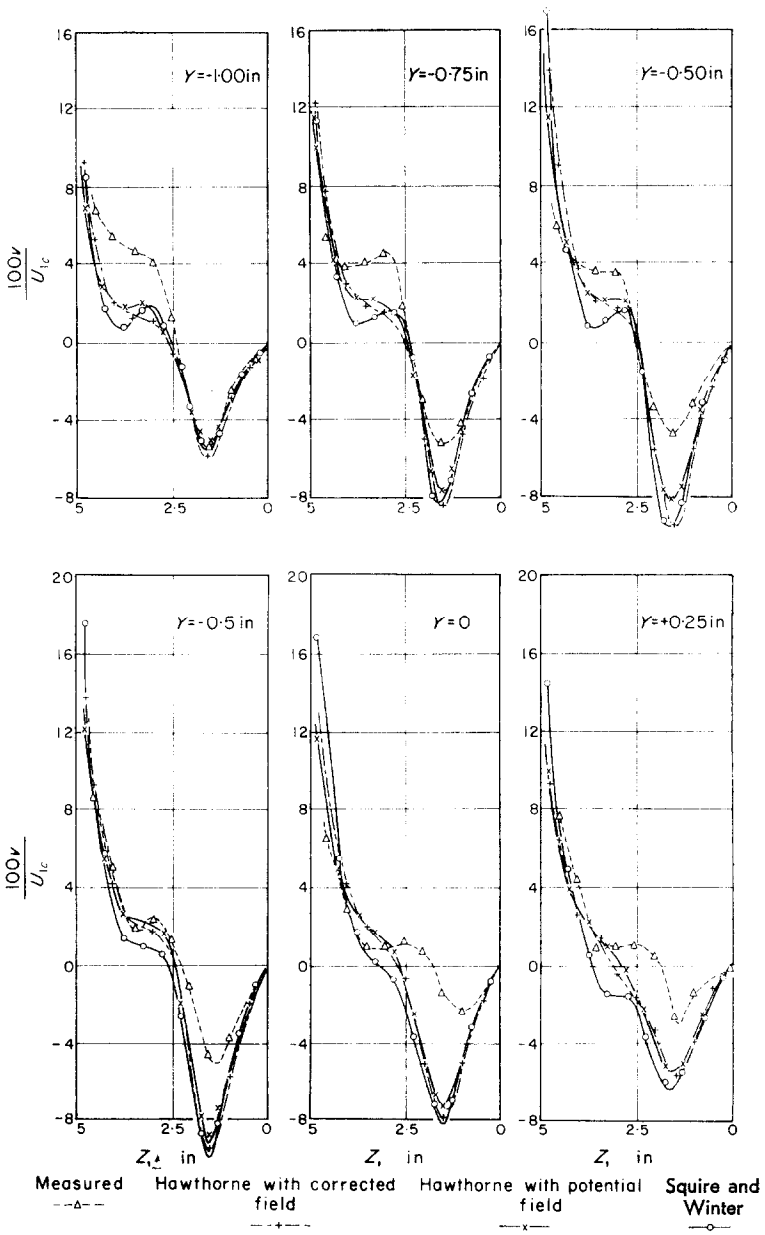

FIG. 21. Component of secondary flow in Y-direction at plane c.

THE TESTING TECHNIQUE

The heat balance between airstream convection and surface heating element first used by Bryant *et al.* [17] for aerofoil tests was employed. Electrical power input to individual strips which run along the span of the blade was adjusted so that the blade surface around the measuring profile was isothermal as judged from thermocouple outputs.

It is assumed that the heat generated electrically is entirely convected away from the surface when obtaining h from

$$q = hA(t_w - t_k)$$

but there are possible errors in this assumption due to the following: conduction to the interior of the blade, conduction along the span due to variation in temperature arising from spanwise variation in heat transfer, and conduction along the chord due to inaccurate setting of the desired isothermal condition. The heating strips were, however, quite thin (0·004 in) and well insulated from the body of the blade, which, being made from wood, was itself reasonably non-conducting. Experiments which were made to estimate the order of the flux to the blade interior and along the span, and from one heater strip to the others along the chord, showed that an error of $\pm 0{\cdot}2$ degC in setting the strip temperature would lead to an error not exceeding 3·3 per cent in calculated heat-transfer coefficient. Estimated probable error from other sources is 3·0 per cent.

DISCUSSION OF RESULTS OF HEAT-TRANSFER MEASUREMENTS

The results shown on Figs. 8–19 will be discussed in two parts: firstly the two-dimensional values of Figs. 8–13, then the modifications produced by the three-dimensional effects shown on Figs. 14–19 are described.

(*i*) *Two-dimensional results*

On the convex surface, for negative and design incidences, the pressure falls steadily to a minimum at $x/c \approx 0{\cdot}7$ where laminar separation followed by turbulent reattachment occurs. The heat-transfer coefficient falls with progressive growth of the layer to the point of laminar separation, where a noticeable local reduction occurs. This is followed by a large increase at the position of turbulent reattachment, and a subsequent rapid tailing-off as this layer thickens in the adverse pressure gradient. The pressure and heat-transfer distributions on the convex surface are comparatively insensitive to incidence changes in this range. For positive incidences, however, a pressure reversal appears near the nose. At incidences of $+10°$ and more this is sufficiently great to promote laminar separation, reattachment (identified by a second peak on the heat-transfer curves) being laminar or turbulent depending on the speed. With the moderate reversal found at $+10°$, laminar reattachment occurs at the two lower speeds ($Re_2 < 3{\cdot}6 \times 10^5$) as shown by the falling heat-transfer coefficient along the convex surface to $x/c \approx 0{\cdot}7$, followed by a rise due to turbulent reattachment, much the same as at negative and design incidences, but at higher speeds the early reattachment is turbulent. At $+20°$ incidence, the increased severity of pressure reversal confines the laminar reattachment to the lowest speed. The distribution of heat transfer over the surface depends strongly on whether or not the initial reattachment is laminar.

On the concave surface, the pressure reversal which occurs near the leading edge at negative incidences persists but with decreasing magnitude as the incidence is increased through the design value to $+10°$. At negative incidences this makes the boundary layer turbulent, as indicated by the peak in the heat-transfer distribution. At zero and $+10°$ incidence, however, the boundary layer remains attached and laminar, as indicated by smoothly-falling curves, to $x/c \approx 0{\cdot}4$. At this point the curves obtained at different Reynolds number start to diverge, but instead of exhibiting the peak and subsequent tailing-off which is characteristic of separation followed by turbulent reattachment, they show a comparatively gradual increase. This anomalous behaviour warrants further study; possibly the boundary layer is intermittently turbulent, or a form of progressive breakdown of the laminar layer is taking place. The particularly low readings of heat transfer obtained at $x/c = 0{\cdot}38$ are known to be due to a local surface irregularity large enough to produce a local separation which initiates the unusual boundary layer behaviour.

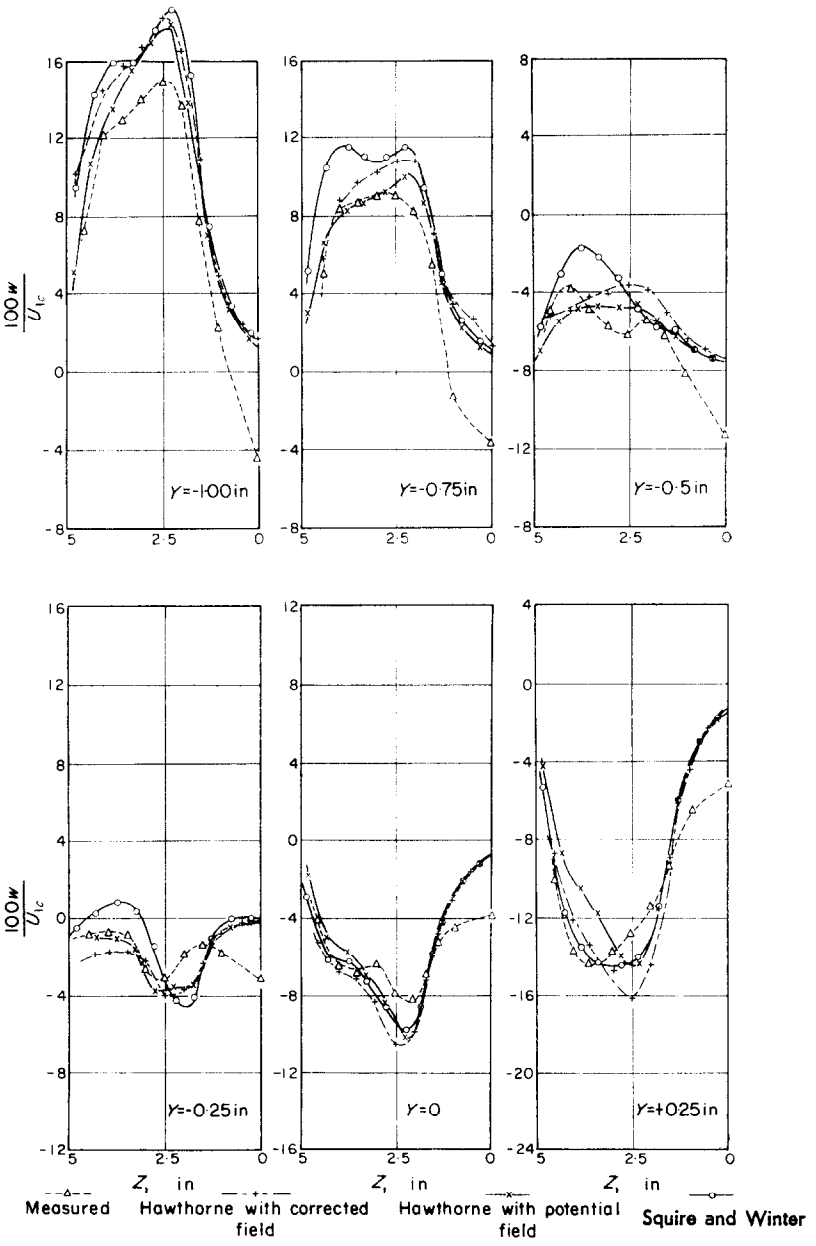

FIG. 22. Component of secondary flow in Z-direction at plane c.

China clay observations on a smooth blade, which did not have this surface irregularity, showed that at positive and design incidences the boundary layer on the concave surface was laminar throughout, and calculation of the heat-transfer coefficient at design incidence shows a steadily falling value of $Nu/(Re_2)^{\frac{1}{2}}$ to 0·32 at the trailing edge. Further calculations with transition assumed at $x/c = 0{\cdot}01$ or at 0·4 did not achieve the measured rate of rise.

(ii) Three-dimensional results

Data were obtained at the 8 stations along the span indicated in Fig. 6 for incidences ranging from $-30°$ to $+20°$. Figures 14–19 give a representative sample of the results at selected stations.

The conditions on the convex surface near the end of the blade span do not vary much with incidence or with Reynolds number, an effect which is due to mixing of low energy air from the boundary layer on the end wall with the flow over the blades near the ends of the span. Armstrong [18] showed separation of the end wall boundary layer in a compressor cascade, leading to separation from the blade surface. At station 8 the blade boundary layer becomes turbulent at $x/c \approx 0{\cdot}4$; at other distances from the wall within the narrow zone subject to this effect, transition will occur at different distances from the leading edge.

At zero incidence the laminar boundary layer on the convex surface survives up to $x/c \approx 0{\cdot}8$ over the remainder of the span. Away from the centre of the span, the general reduction in velocity reduces the ordinates on the graphs, and the cross-flow component of velocity tends to reduce the local dip in heat-transfer rate at the laminar separation point, an effect which is most pronounced towards the ends of the span where the crossflow is most severe (see Fig. 22). A similar state of affairs exists at $-10°$ incidence where the pressure distribution is similar. At $+10°$, $Re_2 = 6{\cdot}45 \times 10^5$, separation followed by turbulent reattachment occurs just downstream of the leading edge near the centre of the span where there is a pressure reversal. This reversal is reduced at successive stations along the span until at station 6 it has just disappeared—an effect due to the successively reduced incidence towards the ends. (The pressure distribution near to the leading edge on the convex surface is particularly sensitive to incidence in the range 0 to $+10°$). For those regions of the blade where the reversal is insufficient to produce separation followed by turbulent reattachment, the laminar layer survives up to $x/c \approx 0{\cdot}7$. For the lower Reynolds number of Fig. 18, the boundary layer remains laminar even over the central part of the span where there is a pressure reversal. The influence of incidence variation along the span is large enough to mask any effect which may be present due to generation of vorticity near the leading edge (such an effect is noted subsequently on the concave surface).

On the concave surface there is a small pressure reversal at zero and $+10°$ incidence which, under two-dimensional conditions, is insufficient to produce separation or transition in the boundary layer. The dependence of heat-transfer coefficients on Reynolds number beyond $x/c \approx 0{\cdot}05$ (seen by comparing Figs. 16 and 17 or Figs. 18 and 19) suggests that, in the presence of secondary flow, transition occurs without separation just behind the leading edge. This was confirmed by china clay tests on a wooden blade, with and without a trip wire at $x/c = 0{\cdot}05$ and by calculation assuming transition at that point. Even with the incidence increased to $+20°$, when there is no detectable pressure reversal at any section along the span, the laminar layer continues to break down towards the end of the span. This may be engendered by severe vorticity generated near the nose of the foil, as noticed by Armstrong [18] in visualization studies on a compressor cascade, where local deflection of the stream can amount to 90° as it passes in an S-bend round the nose. Such vorticity may lead to Goertler type vortices in the boundary layer which could reduce the stability of the layer upstream of the pressure reversal. The pressure reversal on the concave surface at $-10°$ incidence is more severe than at design incidence and leads to laminar separation followed by turbulent reattachment as was the case for two-dimensional results. In these circumstances the destabilizing tendency of the nose vorticity does not influence the general nature of the flow over the concave surface.

The possible influence of increased turbulence

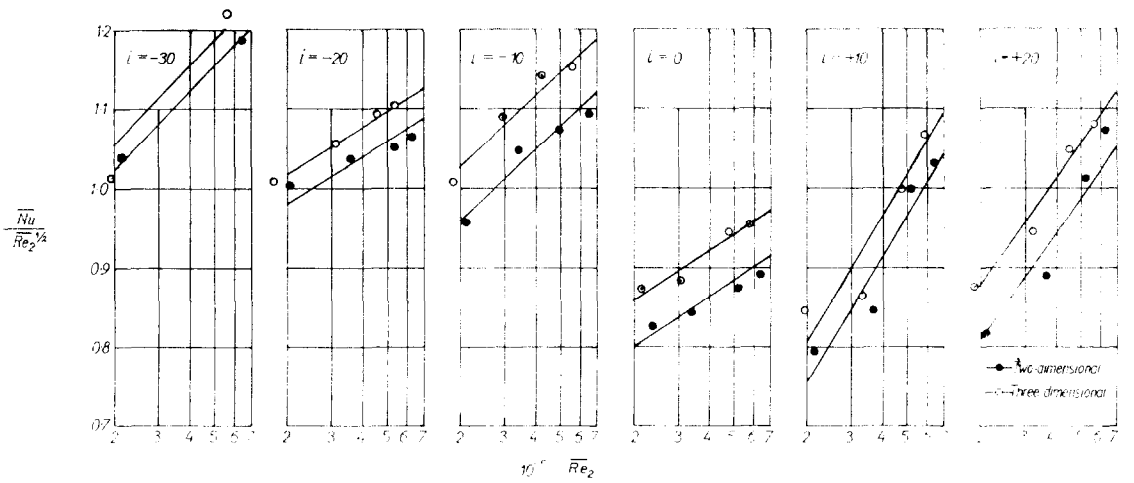

FIG. 23. Comparison of mean heat-transfer coefficients in two- and three-dimensional flow.

due to the velocity spoilers has so far not been mentioned; in the blower-type wind tunnel used, the level of turbulence in the approaching stream without spoilers is known to be already high. Previous tests by Wilson and Pope [1] showed that this was well above the level likely to cause movement of transition from the site of a well-defined pressure minimum, so the influence of increased turbulence due to the flow spoilers is thought to be small.

MEAN HEAT-TRANSFER DATA

Mean heat-transfer coefficients for the whole of the blade surface were computed for conditions of two-dimensional and of three-dimensional flow with the results shown in Fig. 23. The basis of computation was as follows. $\overline{Re}_2$ was based on a mean velocity $\bar{U}_2$ in the downstream plane, defined by

$$\bar{U}_2 = \frac{\int\int U_2 \, dy \, dz}{\int\int dy \, dz}$$

The mean Nusselt number $\overline{Nu}$ over the surface was computed from

$$\overline{Nu} = \frac{\int\int Nu \, dx \, dz}{\int\int dx \, dz}$$

over the blade surface. (At design incidence U_2 was measured by traversing, but at other incidences these traverses were not made, so U_2 was inferred from the equation of continuity and results of velocity traverses in the upstream plane). Whilst the most accurate mean values would be found by integrating Nu_x and U_{xz} over the blade surface, the use of mean quantities as defined above are in convenient terms.

Figure 23 shows an increase of about 6 per cent in mean heat-transfer rate under three-dimensional flow conditions. The straight lines drawn on the graphs are at best only crude approximations to the effect of Reynolds number changes on heat transfer in the complex flow over the blade surfaces, but nevertheless indicate the increase of heat transfer with Reynolds number due to the regions of turbulent boundary layer, and the increase as the incidence moves away from zero.

ACKNOWLEDGEMENTS

The work was sponsored by the Ministry of Supply, and permission to publish the results is gratefully acknowledged. The facilities provided by Dr. J. A. Pope, Head of the Department of Mechanical Engineering at the University of Nottingham at the time of the investigation, and the assistance afforded by the technicians and staff of the Department are also gratefully acknowledged. Valuable assistance was afforded by Dr. P. Eisler of Technograph Electronic Products Limited, who produced the etched foils.

REFERENCES

1. D. G. WILSON and J. A. POPE, Convective heat transfer to gas turbine blade surfaces, *Proc. Inst. Mech. Engrs* **168**, 861 (1954).

2. W. R. HAWTHORNE, Rotational flow through cascades. Pt. I, *Quart. J. Math. Appl. Mech.* **8**, 266 (1955).
3. H. B. SQUIRE and K. G. WINTER, The secondary flow in a cascade of aerofoils in a non-uniform stream, *J. Aero. Sci.* **18**, 271 (1951).
4. T. W. F. BROWN, Some factors in the use of high temperatures in gas turbines, *Proc. Inst. Mech. Engrs* **162**, 167 (1950).
5. D. G. AINLEY, The high temperature turbo-jet engine, *J. Roy. Aero. Soc.* **60**, 563 (1956).
6. D. G. AINLEY, Research on the performance of a type of internally aircooled tubine blade, *Proc. (A) Inst. Mech. Engrs* **167**, 351 (1953).
7. K. W. TODD, Some developments in instrumentation for air-flow analysis. *Proc. Inst. Mech. Engrs* **161**. 213 (1949).
8. E. A. BRIDLE, Some high speed tests on turbine cascades. Nat. Gas Turbine Establishment, Report No. *R.*48 (1949).
9. A. D. S. CARTER, Three-dimensional-flow theories for axial compressors and turbines, *Proc. Inst. Mech. Engrs* **159**, 255 (1948).
10. D. J. K. STUART, Analysis of Reynolds number effects in fluid flow through two dimensional cascades. Aero Res. Coun. *R. & M.* No. 2920 (1955).
11. W. R. HAWTHORNE and W. D. ARMSTRONG, Shear flow through a cascade, *Aero. Quart.* **7**, 247, (1956).
12. H. SCHLICHTING, *Boundary Layer Theory*, 4th. edn., p. 303. McGraw-Hill, New York (1960).
13. S. J. ANDREWS and P. C. BRADLEY, Heat transfer to gas turbine blades. Nat. Gas Turbine Establishment Mem. No. *M.*37 (1948).
14. L. LEES, Stability of the compressible boundary layer in a compressible fluid. *N.A.C.A.* Report No. 876 (1947).
15. E. R. G. ECKERT and W. WEISE, Measurement of temperature distribution on the surface of unheated bodies in high velocity flow. *N.A.C.A.* Tech. Mem. 1000 (1941).
16. H. A. JOHNSON and M. RUBESIN, Aerodynamic heating and convective heat transfer, *Trans. Amer. Soc. Mech. Engrs* **71**, 447 (1949).
17. L. W. BRYANT, E. OWER, A. S. HALLIDAY and V. M. FALKNER, On the convection of heat from the surface of an aerofoil in a wind current. Aero. Res. Counc. *R. & M.* No. 1163 (1928).
18. W. D. ARMSTRONG, Secondary flow in a compressor cascade, *Aero. Quart.* **8**, 240 (1957).

Résumé—En tant que partie d'une étude du transport de chaleur aux aubages de turbine à gaz, les coefficients locaux de transport de chaleur ont été mesurés autour des profils d'une ailette d'une rangée lorsqu'elle est chauffée à quelques degrés au-dessus de la température de l'air en écoulement, chaque profil de mesure étant rendu isotherme. L'écoulement à l'entrée avait des couches limites épaissies artificiellement par des spoilers allant environ à un tiers de l'envergure de l'ailette, de telle façon que de forts écoulements secondaires se sont développés dans l'écoulement dévié.

On a montré que les résultats dans la région d'écoulement uniforme au centre de l'envergure sont virtuellement bidimensionnels. La comparaison avec le travail antérieur de Wilson et Pope [1] montre quelques différences, particulièrement à l'incidence nulle. Un mécanisme important par lequel la variation de la pression totale le long de l'envergure peut augmenter le transport de chaleur, est le mouvement vers l'avant de la transition de la couche limite vers l'endroit d'un renversement de la pression locale près du bord d'attaque de la section, sous condition qu'avec l'écoulement bidimensionnel la couche resterait laminaire après le renversement de pression. Un effet supplémentaire est la contribution des vitesses le long de l'envergure à la surface de l'ailette, produite par les écoulements secondaires, qui augmente le transport de chaleur et le frottement à la paroi. L'augmentation résultante de la vitesse moyenne de transport de chaleur due à la non-uniformité sévère des conditions amont était de 6% pour l'incidence prévue au départ.

Les mesures de l'écoulement secondaire faites entre les ailettes ont été comparées avec les calculs plus ou moins poussés basés sur les méthodes de Hawthorne [2] et de Squire et Winter [3]. La corrélation est raisonnablement bonne dans tous les cas.

Zusammenfassung—Als Teil einer Studie über den Wärmeübergang an die Beschaufelung einer Gasturbine wurden örtliche Wärmeübergangszahlen um Profile einer Schaufel eines Gitters in Sehnenrichtung gemessen, wenn diese um wenige Grad über die Temperatur des Luftstromes erwärmt wurde, wobei an jedem Messprofil der Reihe nach isothermer Zustand vorgegeben wurde. Die Strömung am Eintritt hatte durch Störklappen bis zu ungefähr einem Drittel der Schaufelsehne künstlich verdickte Grenzschichten, so dass starke Sekundärströmungen im umgelenkten Strom entstanden. Es zeigt sich, dass die Ergebnisse über den Bereich gleichförmiger Strömung in der Mitte der Sehne nahezu zweidimensional sind. Ein Vergleich mit der früheren Arbeit von Wilson und Pope [1] zeigt einige Unterschiede, besonders bei der Anstellung Null. Ein bedeutender Mechanismus, der durch eine Veränderung des Gesamtdruckes längs der Sehne den Wärmeübergang zunehmen lassen kann, besteht aus der Vorwärtsbewegung des Grenzschichtüberganges hin zum Punkt der lokalen Druckumkehr nahe an der Profilvorderkante unter der Bedingung, dass bei zweidimensionaler Strömung die Grenzschicht hinter der Druckumkehrstelle laminar bleibt.

Ein weiterer Einfluss wird von den Geschwindigkeiten in Sehnenrichtung an der Schaufeloberfläche

beigetragen, die von den Sekundärströmen, die den Wärmeübergang und die Oberflächenreibung vergrössern, verursacht werden. Die sich ergebende Zunahme des mittleren Wärmeüberganges, die durch die heftige Ungleichförmigkeit der Aufwärtsstrombedingungen hervorgerufen wird, betrug 6 Prozent für die Anstelldaten der Konstruktion.

Messungen der Sekundärströmung, die zwischen den Schaufeln vorgenommen wurden, wurden mit Berechnungen, die auf den Methoden von Hawthorne [2] und Squire und Winter [3] zurückgehen und mit verschiedenen Graden der Verfeinerungen ausgeführt wurden, verglichen.

Die Korrelation ist für alle Fälle annehmbar gut.

Аннотация—Как часть изучения теплообмена газовой турбинной лопатки измерялись локальные коэффициенты теплообмена вдоль хорды профилей одной из лопаток решетки, нагретой на несколько градусов выше температуры обтекающего воздуха, причем каждый измеряемый профиль, в свою очередь, является изотермическим. Поток на входе имел пограничные слои, которые искусственно утолщались закрылками примерно на одну треть размаха лопатки так, что возникали сильные вторичные течения в отклоняющемся потоке.

Показано, что вторичные течения в области однородного потока в центре размаха лопатки действительно являются двумерными. Сравнение с ранее опубликованной работой Уилсона и Попэ [1] показывает некоторые отличия, в частности, при нулевом угле атаки. Одним из важнейших механизмов, с помощью которых изменение полного давления вдоль размаха лопатки может увеличить теплообмен, является перемещение перехода пограничного слоя к точке местного минимума давления вблизи передней кромки поперечного сечения в случае двумерного потока, когда слой остается ламинарным после точки минимума давления; и кроме того, распределение скоростей на поверхности лопатки, вызванное вторичными течениями, которые увеличивают теплообмен и поверхностное трение. Окончательное увелечение средней интенсивности теплообмена за счет строгой неоднородности условий вверх по потоку составляло 6 процента при расчетном угле атаки.

Измерения вторичного течения, проведенные в каналах лопатки, сравнивались с расчетами при различных приближениях, основанных на методах Хоторне [2], Сквайера и Уинтера [3]. Теоретические данные хорошо согласуются с экспериментальными во всех случаях.